

Nonlinear Darcy fluid flow with deposition

V.J. Ervin ^{*} Hyesuk Lee[†] J. Ruiz-Ramírez [‡]

March 23, 2016

Abstract

In this article we consider a model of a filtration process. The process is modeled using the nonlinear Darcy fluid flow equations with a varying permeability, coupled with a deposition equation. Existence and uniqueness of the solution to the modeling equations is established. A numerical approximation scheme is proposed and analyzed, with an a priori error estimate derived. Numerical experiments are presented which support the obtained theoretical results.

Key words. Darcy equation, filtration

AMS Mathematics subject classifications. 65N30

1 Introduction

Filtration processes are ubiquitous in our lives. From oil and fuel filters in engines, to filters used in industrial lines to protect sensitive equipment, to household water filtration systems. In this article we consider the case where the filtration process can be modeled as a fluid flowing through a porous medium. We make the simplifying assumption that the rate of particulate deposition in the filter is only dependent on the porosity and the magnitude of the fluid velocity at that point. Of interest are the modeling equations

$$\frac{\mu_{eff}}{\kappa(\eta)} \mathbf{u} + \nabla p = \mathbf{f}, \text{ in } \Omega, \quad (1.1)$$

$$\nabla \cdot \mathbf{u} = 0, \text{ in } \Omega, \quad (1.2)$$

$$\frac{\partial \eta}{\partial t} + dep(|\mathbf{u}|, \eta) = 0, \text{ in } \Omega, \quad (1.3)$$

subject to suitable boundary and initial conditions. In (1.1)-(1.3) \mathbf{u} and p denote the velocity and pressure of the fluid, respectively, μ_{eff} the effective fluid viscosity, and η and $\kappa(\eta)$ represent the porosity and permeability throughout the filter (Ω), respectively. (A discussion of the model follows in Section 2.)

^{*}Department of Mathematical Sciences, Clemson University, Clemson, SC 29634, USA. (vjervin@clemson.edu)

[†]Department of Mathematical Sciences, Clemson University, Clemson, SC 29634-0975, USA (hklee@mail.clemson.edu), Partially supported by the NSF under grant no. DMS-1418960.

[‡]Department of Mathematical Sciences, Clemson University, Clemson, SC 29634, USA. (javier@clemson.edu)

The lack of regularity of the fluid velocity, $\mathbf{u} \in H_{div}(\Omega)$, leads to an open question of the existence of a solution to (1.1)-(1.3). In order to obtain a modeling system of equations for which a solution can be shown to exist, we replace η in (1.1) by an *smoothed* porosity, η^s . The approach of regularizing the model with the introduction of η^s is, in part, motivated by the Darcy fluid flow equations, which can be derived by *averaging*, e.g. volume averaging [20], homogenization [1], mixture theory [17]. Recently in [9] we considered the case of (steady-state) generalized Newtonian fluid flow through a porous medium, modeled by equations (1.1), (1.2), with $\frac{\mu_{eff}}{\kappa(\eta)} \rightarrow \beta(|\mathbf{u}|)$. With the general assumptions that $\beta(\cdot)$ was a positive, bounded, Lipschitz continuous function, bounded away from zero, and with $\beta(|\mathbf{u}|)$ replaced with $\beta(|\mathbf{u}^s|)$, existence of a solution was established. Two smoothing operators for \mathbf{u} were presented. One was a local averaging operator, whereby $\mathbf{u}^s(\mathbf{x})$ is obtained by averaging \mathbf{u} in a neighborhood of \mathbf{x} . The second smoothing operator, which is nonlocal, computes $\mathbf{u}^s(\mathbf{x})$ using a differential filter applied to \mathbf{u} . That is, \mathbf{u}^s is given by the solution to an elliptic differential equation whose right hand side is \mathbf{u} . For establishing the existence of a solution the key property that the smoothing operator needs to satisfy is that it transform a weakly convergent sequence in $L^2(\Omega)$ into a sequence which converges strongly in $L^\infty(\Omega)$.

A similar model to (1.1)-(1.3) arises in the study of single-phase, miscible displacement of one fluid by another in a porous medium. For this problem η would denote a fluid concentration, and the hyperbolic deposition equation (1.3) is replaced by a parabolic transport equation. Existence and uniqueness for this problem has been investigated and established by Feng [10] and Chen and Ewing [7]. Because of the connection of this model to oil extraction, numerical approximation schemes for this problem have been well established. A summary of these methods is discussed in the recent papers by Bartels, Jensen and Müller [4], and Rivière and Walkington [18].

A steady-state nonlinear Darcy fluid flow problem, with a permeability dependent on the pressure was investigated by Azaïez, Ben Belgacem, Bernardi, and Chorfi [2], and Girault, Murat, and Salgado [13]. For the permeability function Lipschitz continuous, and bounded above and below, existence of a solution $(\mathbf{u}, p) \in L^2(\Omega) \times H^1(\Omega)$ was established. Important in handling the nonlinear permeability function, in establishing existence of a solution, was the property that $p \in H^1(\Omega)$. In [2] the authors also investigated a spectral numerical approximation scheme for the nonlinear Darcy problem, assuming an axisymmetric domain Ω . A convergence analysis for the finite element discretization of this problem was given in [13].

Following a discussion of the model in Section 2, existence of a solution to the modeling equations is established in Section 3. An approximation scheme for the filtration model is presented in Section 4, and an a priori error estimate derived. A numerical simulation of the filtration process is presented in Section 5.

2 Discussion of Filtration Model

In this section we discuss the modeling equations we investigate for the filtration process. We assume that the process can be modeled as fluid flowing through a porous medium with a varying permeability. Additionally we assume that the process has a fixed time horizon, T . (For example, for industrial filters the most practical time to change filters is during scheduled maintenance periods. Drivers are encouraged to change the oil filters in their cars every 3000 miles or every three months, whichever comes first.) We use the following parameters/variables to model the process.

$\Omega \subset \mathbb{R}^d$ ($d = 2, 3$) – the region occupied by the filter,

\mathbf{u} – the fluid velocity,

p – the fluid pressure,

η – the porosity of the medium, $0 < \eta < 1$,

κ – the permeability of the medium, $0 < \kappa < \infty$,

μ_{eff} – the effective fluid viscosity,

\mathbf{n} – the unit outer normal to Ω .

We model the fluid flow using the Darcy fluid flow equations:

$$\frac{\mu_{eff}}{\kappa(\eta)} \mathbf{u} + \nabla p = \mathbf{0}, \quad \text{in } \Omega, t \in (0, T], \quad (2.1)$$

$$\nabla \cdot \mathbf{u} = 0, \quad \text{in } \Omega, t \in (0, T]. \quad (2.2)$$

Note: We are assuming that the particulate is sufficiently sparsely distributed in the fluid that the conservation of mass equation (2.2) is still a valid approximation for the model.

Relationship between permeability κ and porosity η

As $\eta \rightarrow 0$ the “porous” medium transitions to a “solid” medium, in which case the permeability, $\kappa \rightarrow 0$. As $\eta \rightarrow 1$ the medium’s resistance to the flow goes to zero, i.e., its permeability goes to infinity, and the modeling equations are no longer appropriate to describe the fluid flow.

There are a number of postulated models for the relationship between κ and η . The most commonly cited is the Blake-Kozeny model [5]

$$\kappa(\eta) = \frac{D_p^2 \eta^3}{150 (1 - \eta)^2}, \quad (2.3)$$

where D_p represents a material constant – the diameter of the particles comprising the porous medium.

Remark: The permeability of granite is $\approx 10^{-3} - 10^{-4}$ millidarcy. In a filtering process the permeability throughout Ω will always be greater than that of granite. So, it is reasonable to assume that $\kappa(\eta)$ is bounded from below. At the beginning of the filtering process there is a prescribed permeability (porosity) throughout Ω . As the filtering process decreases the permeability (porosity) throughout Ω it is also reasonable to assume that $\kappa(\eta)$ is bounded from above.

2.1 Modeling the deposition

The deposition on the particulate in the filter is modeled by an equation describing the change of porosity. We assume that $\partial\eta(\mathbf{x}, t)/\partial t$ is a function of the magnitude of the velocity and the porosity, i.e.,

$$\frac{\partial\eta}{\partial t} + dep(|\mathbf{u}|, \eta) = 0, \quad \text{in } \Omega, t \in (0, T]. \quad (2.4)$$

As a first approximation, we assume that the deposition function $dep(\cdot, \cdot)$ is a separable function of $|\mathbf{u}|$ and η ,

$$dep(|\mathbf{u}|, \eta) = g(|\mathbf{u}|) h(\eta), \quad \text{in } \Omega, t \in (0, T]. \quad (2.5)$$

The function $g(\cdot)$

We assume that if the fluid is flowing too quickly there is little opportunity for the particles within

the fluid to be captured by the filter. Therefore, beyond a critical value for $|\mathbf{u}|$, say s_c , $g(|\mathbf{u}|)$ is a monotonically decreasing function of $|\mathbf{u}|$. If $|\mathbf{u}|$ is very small then, given that we are modeling a sparsely distributed particulate in the fluid, the rate of deposition will also be very small due to the amount of particulate passing through the filter. In consideration of the about two situations, we postulate that $g(|\mathbf{u}|)$ is a Lipschitz continuous, non-negative, unimodal function, with maximum value occurring at $|\mathbf{u}| = s_c$. A typical profile for $g(\cdot)$ is given in Figure 2.1.

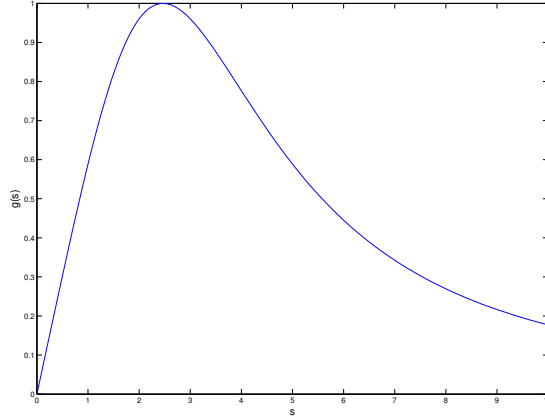


Figure 2.1: Typical profile for $g(\cdot)$.

The function $h(\cdot)$

We assume that as the porosity decreases the rate at which deposition occurs also decreases. This corresponds to the situation that as the deposition occurs (i.e., the porosity decreases) there is less of the filter available for the particulate to adhere to. Based on this, we assume that $h(\eta)$ is a continuous, non-negative, increasing function. Two simple models for $h(\eta)$ are:

$$h(\eta) = \eta \longrightarrow \eta(\mathbf{x}, t) = \eta_0(\mathbf{x}) \exp\left(-\int_0^t g(|\mathbf{u}(\mathbf{x}, s)|) ds\right), \quad (2.6)$$

$$h(\eta) = \eta^r, \quad r > 1, \longrightarrow \eta(\mathbf{x}, t) = \frac{\eta_0(\mathbf{x})}{\left(1 + (r-1)\eta_0(\mathbf{x})^{r-1} \int_0^t g(|\mathbf{u}(\mathbf{x}, s)|) ds\right)^{1/(r-1)}}, \quad (2.7)$$

where, $\eta_0(\mathbf{x})$ denotes the initial porosity distribution throughout the filter.

2.2 Boundary conditions

We assume that the boundary of the filter, $\partial\Omega$, is made up of three parts: an inflow region, Γ_{in} , an outflow region, Γ_{out} and the “walls of the filter,” Γ , i.e., $\partial\Omega = \overline{\Gamma_{in}} \cup \overline{\Gamma_{out}} \cup \overline{\Gamma}$. For well-posedness, equations (2.1)-(2.2) require a scalar boundary condition (typically $\mathbf{u} \cdot \mathbf{n}$ or p) be specified on $\partial\Omega$.

Inflow boundary condition

Two physically reasonable boundary conditions to consider on Γ_{in} are

$$-\mathbf{u} \cdot \mathbf{n} = g_{in} \text{ and} \quad (2.8)$$

$$p = p_{in}. \quad (2.9)$$

Condition (2.8) specifies the flow profile at the inflow boundary, whereas (2.9) corresponds to a specified pressure head along the inflow.

Outflow boundary condition

The fluid outflow profile will be affected by the deposition occurring in the filter. Therefore specifying an outflow profile is not reasonable for this problem. Rather, at the outflow boundary we assume a specified pressure

$$p = p_{out}, \text{ on } \Gamma_{out}. \quad (2.10)$$

Wall boundary condition

Along the walls of the filter we assume a no penetration condition, specifically

$$\mathbf{u} \cdot \mathbf{n} = 0, \text{ on } \Gamma. \quad (2.11)$$

For the mathematical analysis of this problem it is convenient to have homogeneous boundary conditions. This is achieved by introducing a suitable change of variables. For example, in case the specified boundary conditions are

$$-\mathbf{u} \cdot \mathbf{n} = g_{in} \text{ on } \Gamma_{in}, \quad \mathbf{u} \cdot \mathbf{n} = 0 \text{ on } \Gamma, \quad p = p_{out} \text{ on } \Gamma_{out},$$

we introduce functions $\mathbf{u}_b(\mathbf{x}, t)$ (see [11]) and $p_b(\mathbf{x}, t)$ defined on $\bar{\Omega}$ satisfying

$$\begin{aligned} \nabla \cdot \mathbf{u}_b &= 0, \text{ in } \Omega \times (0, T], \\ \mathbf{u}_b \cdot \mathbf{n} &= -g_{in}, \text{ on } \Gamma_{in} \times (0, T], \\ \mathbf{u}_b \cdot \mathbf{n} &= \int_{\Gamma_{in}} g_{in}(s) ds / |\Gamma_{out}|, \text{ on } \Gamma_{out} \times (0, T], \\ \mathbf{u}_b \cdot \mathbf{t}_i &= 0, \text{ on } \Gamma_{in} \times (0, T], \\ \mathbf{u}_b &= \mathbf{0}, \text{ on } \partial\Omega \setminus (\Gamma_{in} \cup \Gamma_{out}) \times (0, T], \end{aligned} \quad \begin{aligned} -\Delta p_b &= 0, \text{ in } \Omega \times (0, T], \\ p_b &= p_{out}, \text{ on } \Gamma_{out} \times (0, T], \\ \frac{\partial p_b}{\partial \mathbf{n}} &= 0, \text{ on } \partial\Omega \setminus \Gamma_{out} \times (0, T]. \end{aligned}$$

where t_i , $i = 1, \dots, (d-1)$ denotes an orthogonal set of tangent vectors on Γ_{in} , and $|\Gamma_{out}|$ the measure of Γ_{out} with respect to ds .

(In case the pressure is specified on the inflow boundary Γ_{in} then $\mathbf{u}_b = \mathbf{0}$ and the definition of p_b is appropriately modified.)

With the change of variables: $\mathbf{u} = \mathbf{u}_a + \mathbf{u}_b$ and $p = p_a + p_b$ we obtain the following system of

modeling equations for the filtration process:

$$\frac{\mu_{eff}}{\kappa(\eta)} \mathbf{u}_a + \frac{\mu_{eff}}{\kappa(\eta)} \mathbf{u}_b + \nabla p_a = -\nabla p_b, \text{ in } \Omega \times (0, T], \quad (2.12)$$

$$\nabla \cdot \mathbf{u}_a = 0, \text{ in } \Omega \times (0, T], \quad (2.13)$$

$$\frac{\partial \eta}{\partial t} + g(|\mathbf{u}_a + \mathbf{u}_b|) h(\eta) = 0, \text{ in } \Omega \times (0, T], \quad (2.14)$$

$$\mathbf{u}_a \cdot \mathbf{n} = 0, \text{ on } \Gamma_{in} \cup \Gamma \times (0, T], \quad (2.15)$$

$$p_a = 0, \text{ on } \Gamma_{out} \times (0, T], \quad (2.16)$$

$$\eta(\mathbf{x}, 0) = \eta_0(\mathbf{x}) \text{ in } \Omega. \quad (2.17)$$

To simplify the notation, we let $\mathbf{b} = \mathbf{u}_b$, $\mathbf{f} = -\nabla p_b$, $\beta(\eta) = \mu_{eff}/\kappa(\eta)$, and drop the a subscript on \mathbf{u}_a and p_a to obtain

$$\beta(\eta) \mathbf{u} + \beta(\eta) \mathbf{b} + \nabla p = \mathbf{f}, \text{ in } \Omega \times (0, T], \quad (2.18)$$

$$\nabla \cdot \mathbf{u} = 0, \text{ in } \Omega \times (0, T], \quad (2.19)$$

$$\frac{\partial \eta}{\partial t} + g(|\mathbf{u} + \mathbf{b}|) h(\eta) = 0, \text{ in } \Omega \times (0, T], \quad (2.20)$$

$$\mathbf{u} \cdot \mathbf{n} = 0, \text{ on } \Gamma_{in} \cup \Gamma \times (0, T], \quad (2.21)$$

$$p = 0, \text{ on } \Gamma_{out} \times (0, T], \quad (2.22)$$

$$\eta(\mathbf{x}, 0) = \eta_0(\mathbf{x}) \text{ in } \Omega. \quad (2.23)$$

Remark: $\beta(\eta)$ is implicitly a function of \mathbf{x} through the dependence of η on \mathbf{x} .

In the next section we show that, under suitable assumptions on $\beta(\cdot)$, there exists a solution to (2.18)-(2.23).

3 Existence and Uniqueness

In this section we investigate the existence and uniqueness of solutions to the nonlinear system equations (2.18)-(2.23). We assume that $\Omega \subset \mathbb{R}^d$, $d = 2$ or 3 , is a convex polyhedral domain and for vectors in \mathbb{R}^d $|\cdot|$ denotes the Euclidean norm.

Weak formulation of (2.18)-(2.23)

Let $H_{div}(\Omega) = \{\mathbf{v} \in L^2(\Omega) : \nabla \cdot \mathbf{v} \in L^2(\Omega)\}$, and $X = \{\mathbf{v} \in H_{div}(\Omega) : \mathbf{v} \cdot \mathbf{n} = 0 \text{ on } \Gamma_{in} \cup \Gamma\}$. Define the bilinear form $b(\cdot, \cdot)$ and the div-free subspace, Z , of X as

$$b : X \times L^2(\Omega) \longrightarrow \mathbb{R}, \quad b(\mathbf{v}, q) := \int_{\Omega} q \nabla \cdot \mathbf{v} d\Omega, \\ Z := \{\mathbf{v} \in X : b(\mathbf{v}, q) = 0, \forall q \in L^2(\Omega)\}.$$

We use

$$(f, g) := \int_{\Omega} f \cdot g d\Omega, \quad \text{and} \quad \|f\| := (f, f)^{1/2}$$

to denote the L^2 inner product and the L^2 norm over Ω , respectively, for both scalar and vector valued functions.

Additionally, we introduce the norm

$$\|\mathbf{v}\|_X = \left(\int_{\Omega} (\nabla \cdot \mathbf{v} \nabla \cdot \mathbf{v} + \mathbf{v} \cdot \mathbf{v}) d\Omega \right)^{1/2}.$$

Remark: For $\mathbf{v} \in H_{div}(\Omega)$ it follows that $\mathbf{v} \cdot \mathbf{n} \in H^{-1/2}(\partial\Omega)$. For the interpretation of the condition $\mathbf{v} \cdot \mathbf{n} = 0$ on $\Gamma_{in} \cup \Gamma$ see [12, 19].

We make the following assumptions on $\beta(\cdot)$, $g(\cdot)$ and $h(\cdot)$.

Assumptions on $\beta(\cdot)$

A β 1: $\beta(\cdot) : \mathbb{R}^+ \rightarrow \mathbb{R}^+$,

A β 2: $0 < \beta_{min} \leq \beta(s) \leq \beta_{max}, \forall s \in \mathbb{R}^+$,

A β 3: β is Lipschitz continuous, $|\beta(s_1) - \beta(s_2)| \leq \beta_{Lip} |s_1 - s_2|$.

Assumptions on $g(\cdot)$

A g 1: $g(\cdot) : \mathbb{R}^+ \cup \{0\} \rightarrow \mathbb{R}^+ \cup \{0\}$,

A g 2: $g(s) \leq g_{max}, \forall s \in \mathbb{R}^+ \cup \{0\}$,

A g 3: g is Lipschitz continuous, $|g(s_1) - g(s_2)| \leq g_{Lip} |s_1 - s_2|$.

Assumptions on $h(\cdot)$

A h 1: $h(\cdot) : \mathbb{R}^+ \rightarrow \mathbb{R}^+ \cup \{0\}$,

A h 2: $h(s) \leq h_{max}, \forall s \in \mathbb{R}^+$,

A h 3: h is Lipschitz continuous, $|h(s_1) - h(s_2)| \leq h_{Lip} |s_1 - s_2|$.

Remark: The assumptions on β , g , and h are consistent with the discussion in Section 2.1. Note that g_{max} , h_{max} should be given to guarantee positivity of the porosity ($0 < \eta$) for some finite time interval.

Assumptions on η^s

A η^s 1. For $\eta(\cdot, t) \in L^2(\Omega)$, $\|\eta^s(t)\|_{L^\infty(\Omega)} \leq C_s \|\eta(t)\|_{L^2(\Omega)}$,

A η^s 2. The mapping $\eta(\cdot, t) \mapsto \eta^s(\cdot, t)$ is linear.

Two smoothers which satisfy **A η^s 1** and **A η^s 2** are discussed in [9]. One is a local averaging operator and the other a differential smoothing operator.

We assume that \mathbf{b} and \mathbf{f} are continuous with respect to t on the interval $(0, T)$ and have a continuous extension to the interval $(0 - \delta, T)$ for some $\delta > 0$, i.e., $\mathbf{b}, \mathbf{f} \in C^0(0^-, T; L^2(\Omega))$.

We restate (2.18)-(2.23) as: *Given $\eta_0(\mathbf{x}) \in L^2(\Omega)$, $\mathbf{b}, \mathbf{f} \in C^0(0^-, T; L^2(\Omega)) \cap L^\infty(0, T; L^2(\Omega))$, find $(\mathbf{u}, p) \in L^2(0, T; X) \times L^2(0, T; L^2(\Omega))$, $\eta \in H^1(0, T; L^2(\Omega))$ such that for a.e. t , $0 < t < T$,*

$$(\beta(\eta^s)\mathbf{u}, \mathbf{v}) + (\beta(\eta^s)\mathbf{b}, \mathbf{v}) - b(\mathbf{v}, p) = (\mathbf{f}, \mathbf{v}), \forall \mathbf{v} \in X, \quad (3.1)$$

$$b(\mathbf{u}, q) = 0, \forall q \in L^2(\Omega), \quad (3.2)$$

$$\left(\frac{\partial \eta}{\partial t}, \xi \right) + (g(|\mathbf{u} + \mathbf{b}|)h(\eta), \xi) = 0, \forall \xi \in L^2(\Omega). \quad (3.3)$$

For the spaces X and $L^2(\Omega)$ we have the following inf-sup condition

$$\inf_{q \in L^2(\Omega)} \sup_{\mathbf{v} \in X} \frac{b(\mathbf{v}, q)}{\|q\| \|\mathbf{v}\|_X} \geq c_0 > 0. \quad (3.4)$$

In view of the inf-sup condition we can restate (3.1)-(3.3) as: *Given $\eta_0(\mathbf{x}) \in L^2(\Omega)$, $\mathbf{b}, \mathbf{f} \in C^0(0^-, T; L^2(\Omega)) \cap L^\infty(0, T; L^2(\Omega))$, find $\mathbf{u} \in L^2(0, T; Z)$, $\eta \in H^1(0, T; L^2(\Omega))$ such that for a.e. t , $0 < t < T$,*

$$(\beta(\eta^s)\mathbf{u}, \mathbf{v}) + (\beta(\eta^s)\mathbf{b}, \mathbf{v}) = (\mathbf{f}, \mathbf{v}), \forall \mathbf{v} \in Z, \quad (3.5)$$

$$\left(\frac{\partial \eta}{\partial t}, \xi\right) + (g(|\mathbf{u} + \mathbf{b}|)h(\eta), \xi) = 0, \forall \xi \in L^2(\Omega). \quad (3.6)$$

Introduce the bounded Darcy projection operator: $\mathcal{P}_\eta : L^2(\Omega) \rightarrow Z$ defined by $\mathbf{z} := \mathcal{P}_\eta(\mathbf{r})$ where,

$$\begin{aligned} (\beta(\eta^s)\mathbf{z}, \mathbf{v}) - b(\mathbf{v}, \lambda) &= (\mathbf{r}, \mathbf{v}), \forall \mathbf{v} \in X, \\ b(\mathbf{z}, q) &= 0, \forall q \in L^2(\Omega). \end{aligned}$$

That \mathcal{P}_η is well defined follows from **A β 1-A β 3**. Note that \mathbf{u} in (3.5) may be written as

$$\mathbf{u} = \mathcal{P}_\eta(\mathbf{f} - \beta(\eta^s)\mathbf{b}). \quad (3.7)$$

Additionally, from (3.5) with the choice $\mathbf{v} = \mathbf{u}$, it is straight forward to see that

$$\begin{aligned} \|\mathbf{u}(t)\| &= \|\mathbf{u}(t)\|_X \leq \frac{1}{\beta_{min}}(\|\mathbf{f}(t)\| + \beta_{max}\|\mathbf{b}(t)\|) \\ &\leq \frac{1}{\beta_{min}}(\|\mathbf{f}\|_{L^\infty(0, T; L^2(\Omega))} + \beta_{max}\|\mathbf{b}\|_{L^\infty(0, T; L^2(\Omega))}). \end{aligned} \quad (3.8)$$

Using \mathcal{P}_η we can restate (3.5), (3.6) as: *Given $\eta_0(\mathbf{x}) \in L^2(\Omega)$, $\mathbf{b}, \mathbf{f} \in C^0(0^-, T; L^2(\Omega)) \cap L^\infty(0, T; L^2(\Omega))$, find $\eta \in H^1(0, T; L^2(\Omega))$ such that for a.e. t , $0 < t < T$,*

$$\left(\frac{\partial \eta}{\partial t}, \xi\right) + (g(|\mathcal{P}_\eta(\mathbf{f} - \beta(\eta^s)\mathbf{b}) + \mathbf{b}|)h(\eta), \xi) = 0, \forall \xi \in L^2(\Omega). \quad (3.9)$$

We recall the Picard-Lindelöf Theorem. (Also know as the Cauchy-Lipschitz Theorem).

Theorem 3.1 ([14], Theorem I.3.1) *Let I denote a domain in \mathbb{R} containing the point t_0 , Y a Banach space and $f : \mathbb{R} \times Y \rightarrow Y$. Suppose that f is continuous in its first variable and locally Lipschitz continuous in its second variable. Then, there exists $\epsilon > 0$ such that the initial value problem*

$$u' = f(t, u), \quad (3.10)$$

$$u(t_0) = u_0, \quad (3.11)$$

has a unique solution in $C^0(t_0 - \epsilon, t_0 + \epsilon; Y)$.

Let $\mathcal{F}(t, \eta) = g(|\mathcal{P}_\eta(\mathbf{f} - \beta(\eta^s)\mathbf{b}) + \mathbf{b}|)h(\eta)$. The continuity of \mathcal{F} with respect to t follows from the continuity of \mathbf{f} and \mathbf{b} with respect to t , the boundedness of \mathcal{P}_η , and the continuity of g . To

investigate the local Lipschitz continuity of \mathcal{F} with respect to η consider the following.

$$\begin{aligned}
\|\mathcal{F}(t, \eta_1) - \mathcal{F}(t, \eta_2)\| &= \|g(|\mathcal{P}_{\eta_1}(\mathbf{f} - \beta(\eta_1^s)\mathbf{b}) + \mathbf{b}|)h(\eta_1) - g(|\mathcal{P}_{\eta_2}(\mathbf{f} - \beta(\eta_2^s)\mathbf{b}) + \mathbf{b}|)h(\eta_2)\| \\
&\leq \|g(|\mathcal{P}_{\eta_1}(\mathbf{f} - \beta(\eta_1^s)\mathbf{b}) + \mathbf{b}|)(h(\eta_1) - h(\eta_2))\| \\
&\quad + \|(g(|\mathcal{P}_{\eta_1}(\mathbf{f} - \beta(\eta_1^s)\mathbf{b}) + \mathbf{b}|) - g(|\mathcal{P}_{\eta_2}(\mathbf{f} - \beta(\eta_2^s)\mathbf{b}) + \mathbf{b}|)h(\eta_2)\| \\
&\leq g_{max} \|h(\eta_1) - h(\eta_2)\| \\
&\quad + g_{Lip} \|(|\mathcal{P}_{\eta_1}(\mathbf{f} - \beta(\eta_1^s)\mathbf{b}) + \mathbf{b}| - |\mathcal{P}_{\eta_2}(\mathbf{f} - \beta(\eta_2^s)\mathbf{b}) + \mathbf{b}|)h(\eta_2)\| \\
&\leq g_{max} h_{Lip} \|\eta_1 - \eta_2\| \\
&\quad + g_{Lip} \|(\mathcal{P}_{\eta_1}(\mathbf{f} - \beta(\eta_1^s)\mathbf{b}) - \mathcal{P}_{\eta_2}(\mathbf{f} - \beta(\eta_2^s)\mathbf{b}))h(\eta_2)\| \\
&\leq g_{max} h_{Lip} \|\eta_1 - \eta_2\| \\
&\quad + g_{Lip} h_{max} \|\mathcal{P}_{\eta_1}(\mathbf{f} - \beta(\eta_1^s)\mathbf{b}) - \mathcal{P}_{\eta_2}(\mathbf{f} - \beta(\eta_2^s)\mathbf{b})\|. \tag{3.12}
\end{aligned}$$

Now, with $\mathbf{u}_1 = \mathcal{P}_{\eta_1}(\mathbf{f} - \beta(\eta_1^s)\mathbf{b}) \in Z$ and $\mathbf{u}_2 = \mathcal{P}_{\eta_2}(\mathbf{f} - \beta(\eta_2^s)\mathbf{b}) \in Z$ we have that

$$(\beta(\eta_1^s)\mathbf{u}_1, \mathbf{v}) = (\mathbf{f}, \mathbf{v}) - (\beta(\eta_1^s)\mathbf{b}, \mathbf{v}), \quad \forall \mathbf{v} \in Z, \tag{3.13}$$

$$\text{and } (\beta(\eta_2^s)\mathbf{u}_2, \mathbf{v}) = (\mathbf{f}, \mathbf{v}) - (\beta(\eta_2^s)\mathbf{b}, \mathbf{v}), \quad \forall \mathbf{v} \in Z. \tag{3.14}$$

Subtracting (3.14) from (3.13), and with the choice $\mathbf{v} = \mathbf{u}_1 - \mathbf{u}_2$, yields

$$(\beta(\eta_1^s)(\mathbf{u}_1 - \mathbf{u}_2), (\mathbf{u}_1 - \mathbf{u}_2)) = ((\beta(\eta_2^s) - \beta(\eta_1^s))\mathbf{u}_2, (\mathbf{u}_1 - \mathbf{u}_2)) + ((\beta(\eta_2^s) - \beta(\eta_1^s))\mathbf{b}, (\mathbf{u}_1 - \mathbf{u}_2)).$$

Hence, with (3.8),

$$\begin{aligned}
\beta_{min}\|\mathbf{u}_1 - \mathbf{u}_2\| &\leq \beta_{Lip} \|\eta_2^s - \eta_1^s\| \|\mathbf{u}_2\| + \beta_{Lip} \|\eta_2^s - \eta_1^s\| \|\mathbf{b}\| \\
&\leq \beta_{Lip} (\|\mathbf{u}_2\| + \|\mathbf{b}\|) \|\eta_2^s - \eta_1^s\|_{\infty} \\
&\leq \beta_{Lip} \left(\frac{1}{\beta_{min}} \|\mathbf{f}\| + \frac{\beta_{max}}{\beta_{min}} \|\mathbf{b}\| + \|\mathbf{b}\| \right) C_s \|\eta_2 - \eta_1\|.
\end{aligned}$$

Thus we obtain

$$\begin{aligned}
\|\mathcal{P}_{\eta_1}(\mathbf{f} - \beta(\eta_1^s)\mathbf{b}) - \mathcal{P}_{\eta_2}(\mathbf{f} - \beta(\eta_2^s)\mathbf{b})\| &= \|\mathbf{u}_1 - \mathbf{u}_2\| \\
&\leq C_s \frac{\beta_{Lip}}{\beta_{min}^2} (\|\mathbf{f}\| + (\beta_{max} + \beta_{min})\|\mathbf{b}\|) \|\eta_2 - \eta_1\|. \tag{3.15}
\end{aligned}$$

Combining (3.12) and (3.15), we have

$$\|\mathcal{F}(t, \eta_1) - \mathcal{F}(t, \eta_2)\| \leq \mathcal{F}_{Lip} \|\eta_2 - \eta_1\|, \quad \text{where} \tag{3.16}$$

$$\mathcal{F}_{Lip} = g_{max} h_{Lip} \tag{3.17}$$

$$+ C_s \frac{\beta_{Lip}}{\beta_{min}^2} g_{Lip} h_{max} (\|\mathbf{f}\|_{L^{\infty}(0,T;L^2(\Omega))} + (\beta_{max} + \beta_{min})\|\mathbf{b}\|_{L^{\infty}(0,T;L^2(\Omega))}). \tag{3.18}$$

Then, from Theorem 3.1, we have that there exists $\epsilon > 0$ such that there exists a unique solution $\eta \in C^0(0, \epsilon; L^2(\Omega))$ to (3.9).

Regarding the additional regularity of η , formally taking ξ equal to $\partial\eta/\partial t$ in (3.9) we have

$$\begin{aligned}
\left\| \frac{\partial\eta}{\partial t} \right\|^2 &\leq \|g(|\mathcal{P}_{\eta}(\mathbf{f} - \beta(\eta^s)\mathbf{b}) + \mathbf{b}|)h(\eta)\| \left\| \frac{\partial\eta}{\partial t} \right\| \\
\Rightarrow \left\| \frac{\partial\eta}{\partial t} \right\| &\leq g_{max} h_{max} |\Omega|. \tag{3.19}
\end{aligned}$$

Using the established fact that $\eta \in C^0(0, \epsilon; L^2(\Omega))$, it then follows that $\eta \in H^1(0, \epsilon; L^2(\Omega))$. In order to establish this result rigorously, we consider a Galerkin approximation of (3.9) in which the approximation of $\partial\eta/\partial t$ does indeed lie in $L^2(0, \epsilon; L^2(\Omega))$ and then taking the limit.

Next, note that $\|\mathcal{F}(t, \eta)\| \leq g_{max} h_{max} |\Omega|^{1/2}$. Hence both $\mathcal{F}(t, \eta)$ and its Lipschitz constant with respect to η are bounded independent of t and η . Then, from the proof of Theorem 3.1 (see [14]), ϵ may be chosen such that $0 < \epsilon < 1/\mathcal{F}_{Lip}$. As $\epsilon > 0$ can be chosen independent of t and η , the solution can be extended to $0 < t < T$.

We summarize the above discussion in the following theorem.

Theorem 3.2 *For $\beta(\cdot)$ satisfying **A β 1–A β 3**, $g(\cdot)$ satisfying **Ag1–Ag3**, $h(\cdot)$ satisfying **Ah1–Ah3**, and $\eta(\cdot)$ satisfying **A η 1–A η 2**, given $\eta_0(\mathbf{x}) \in L^2(\Omega)$, $\mathbf{b}, \mathbf{f} \in C^0(0^-, T; L^2(\Omega)) \cap L^\infty(0, T; L^2(\Omega))$, there exists a unique solution $(\mathbf{u}, p) \in L^2(0, T; X) \times L^2(0, T; L^2(\Omega))$, $\eta \in H^1(0, T; L^2(\Omega))$ satisfying (3.1)–(3.3), for a.e. t , $0 < t < T$.*

Remark: Important in establishing the existence and uniqueness of the solution is the assumption that $\beta(\mathbf{x}, t) \geq \beta_{min}$. Under the deposition process eventually (assuming that the mathematical equations correctly model the physical problem), after some finite time, this assumption is violated.

4 Finite element approximation

In this section we investigate the finite element approximation to *Given $\eta_0(\mathbf{x}) \in L^2(\Omega)$, $\mathbf{b}, \mathbf{f} \in C^0(0^-, T; L^2(\Omega)) \cap L^\infty(0, T; L^2(\Omega))$, find $(\mathbf{u}, p) \in L^2(0, T; X) \times L^2(0, T; L^2(\Omega))$, $\eta \in H^1(0, T; L^2(\Omega))$ such that for a.e. t , $0 < t < T$,*

$$(\beta(\eta^s)\mathbf{u}, \mathbf{v}) + (\beta(\eta^s)\mathbf{b}, \mathbf{v}) - b(\mathbf{v}, p) = (\mathbf{f}, \mathbf{v}), \quad \forall \mathbf{v} \in X, \quad (4.1)$$

$$b(\mathbf{u}, q) = 0, \quad \forall q \in L^2(\Omega), \quad (4.2)$$

$$\left(\frac{\partial\eta}{\partial t}, \xi\right) + (g(|\mathbf{u} + \mathbf{b}|)\eta, \xi) = 0, \quad \forall \xi \in L^2(\Omega). \quad (4.3)$$

Note that with regard to the general modeling equations (2.18)–(2.23), here we have chosen $h(\eta) = \eta$.

As before, let $\Omega \subset \mathbb{R}^d$ denote a convex polygonal or polyhedral domain and let \mathcal{T}_h be a triangulation of Ω made either of triangles or quadrilaterals in \mathbb{R}^2 or tetrahedra or hexahedra in \mathbb{R}^3 . Thus, the computational domain is defined by $\Omega = \bigcup_{K \in \mathcal{T}_h} K$. We assume that there exist constants c_1, c_2 such that $c_1 h \leq h_K \leq c_2 \rho_K$, where h_K is the diameter of the cell K , ρ_K is the diameter of the biggest neighborhood included in K , and $h = \max_{K \in \mathcal{T}_h} h_K$. For $k \in \mathbb{N}$, let

$$\mathbb{P}_k^T := \text{span}\{x_1^{\alpha_1} x_2^{\alpha_2} \dots x_d^{\alpha_d} : 0 \leq \alpha_1 + \alpha_2 + \dots + \alpha_d \leq k\}, \quad \text{and} \quad (4.4)$$

$$\mathbb{P}_k^Q := \text{span}\{x_1^{\alpha_1} x_2^{\alpha_2} \dots x_d^{\alpha_d} : 0 \leq \alpha_1, \alpha_2, \dots, \alpha_d \leq k\}. \quad (4.5)$$

For K a triangle/tetrahedron in \mathbb{R}^d we let $P_k(K) = \{f : f|_K \in \mathbb{P}_k^T\}$. For K a quadrilateral/hexahedron in \mathbb{R}^d we let $P_k(K) = \{f : f|_K \in \mathbb{P}_k^Q\}$. $RT_k(\mathcal{T}_h)$ is used to denote the Raviart-

Thomas space of order k [6]. We use the following finite element spaces:

$$\begin{aligned} X_h &= \{RT_k(\mathcal{T}_h) \cap X\}, \quad Q_h = \{q \in L^2(\Omega) : q|_K \in P_k(K), \forall K \in \mathcal{T}_h\}, \\ R_h &= \{r \in L^2(\Omega) : r|_K \in P_m(K), \forall K \in \mathcal{T}_h\}, \quad R_h^s = \{r \in C^0(\Omega) : r|_K \in P_{\max\{1,m\}}(K), \forall K \in \mathcal{T}_h\}, \\ Z_h &= \{\mathbf{v} \in X_h : (q, \mathbf{v}) = 0, \forall q \in Q_h\}. \end{aligned}$$

Note that as $\nabla \cdot X_h \subset Q_h$, for $\mathbf{v} \in Z_h$ we have that $\|\nabla \cdot \mathbf{v}\| = 0$, thus $\|\mathbf{v}\|_X = \|\mathbf{v}\|$. For N given, let $\Delta t = T/N$, and $t_n = n\Delta t$, $n = 0, 1, \dots, N$. Additionally, define

$$d_t f^n := \frac{f^n - f^{n-1}}{\Delta t}, \quad \bar{f}^n := \frac{f^n + f^{n-1}}{2}, \quad \tilde{f}^n := f^{n-1} + \frac{1}{2}f^{n-2} - \frac{1}{2}f^{n-3}.$$

The following norms are used in the analysis

$$\|v\|_\infty := \|v(t)\|_{L^\infty(\Omega)}, \quad \|v\| := \left(\sum_{n=0}^N \|v(t_n)\|^2 \Delta t \right)^{1/2}, \quad \|v\|_\infty := \sup_{0 \leq n \leq N} \|v(t_n)\|_\infty.$$

For the a priori error estimates presented below the solution (\mathbf{u}, p, η) to (4.1)-(4.3) is required to be *sufficiently regular*. The regularity assumptions we assume are, for some $\delta > 0$,

$$\mathbf{u} \in L^\infty(0, T; L^\infty(\Omega)) \cap L^\infty(0, T; H^{k+1}(\Omega)), \quad \mathbf{u}_t \in L^\infty(0, \delta; L^2(\Omega)), \quad \mathbf{u}_{tt} \in L^2(0, T; L^2(\Omega)) \quad (4.6)$$

$$p \in L^\infty(0, T; H^{k+1}(\Omega)), \quad \eta \in L^\infty(0, T; L^\infty(\Omega)) \cap L^\infty(0, T; H^{m+1}(\Omega)) \quad (4.7)$$

$$\eta_t \in L^\infty(0, T; H^{m+1}(\Omega)), \quad \eta_{tt} \in L^2(0, T; L^2(\Omega)) \cap L^\infty(0, \delta; L^2(\Omega)), \quad (4.8)$$

$$\eta_{ttt} \in L^2(0, T; L^2(\Omega)). \quad (4.9)$$

Throughout, we use C to denote a generic nonnegative constant, independent of the mesh parameter h and time step Δt , whose actual value may change from line to line in the analysis.

Initialization of the Approximation Scheme

The approximation scheme described and analyzed below is a three-level scheme. To initialize the procedure suitable approximations are required for \mathbf{u}_h^n for $n = 0, 1, 2$, and for η_h^n for $n = 2$. Here we state our assumptions on these initial approximates. (An initialization procedure is presented in the Appendix of [8].)

$$\|\mathbf{u}^n - \mathbf{u}_h^n\|_X^2 + \|\eta^n - \eta_h^n\|^2 \leq C(\Delta t)^4 + C\left(h^{2k+2} + h^{2m+2}\right), \quad \text{for } n = 0, 1, 2. \quad (4.10)$$

Approximation Scheme

The approximation scheme we investigate is: Given $\eta_0 \in R_h$, for $n = 3, \dots, N$, determine $(\mathbf{u}_h^n, p_h^n, \eta_h^n) \in X_h \times Q_h \times R_h$ satisfying

$$(\beta(\eta_h^{n,s})\mathbf{u}_h^n + \beta(\eta_h^{n,s})\mathbf{b}^n, \mathbf{v}) - (p_h^n, \nabla \cdot \mathbf{v}) = (\mathbf{f}^n, \mathbf{v}), \quad \forall \mathbf{v} \in X_h \quad (4.11)$$

$$(q, \nabla \cdot \mathbf{u}_h^n) = 0, \quad \forall q \in Q_h \quad (4.12)$$

$$(d_t \eta_h^n, r) + (g(|\tilde{\mathbf{u}}_h^n + \mathbf{b}^{n-1/2}|)\bar{\eta}_h^n, r) = 0, \quad \forall r \in R_h, \quad (4.13)$$

where $\mathbf{b}^{n-1/2} := \mathbf{b}(\frac{t^n + t^{n-1}}{2})$.

Regarding $\eta_h^{n,s}$, note that applying a smoother, \mathcal{S} , to a function $\eta_h^n \in R_h$ (typically) does not result in $\eta_h^{n,s} \in R_h^s$. Therefore, we let $\mathcal{S}(\eta_h^n) \in H^{m+1}(\Omega) \cap C^0(\Omega)$ denote the result of the smoother applied to η_h^n , and define

$$\eta_h^{n,s}(x) = I_h \mathcal{S}(\eta_h^n)(x), \quad (4.14)$$

where $I_h : C^0(\Omega) \rightarrow R_h^s$ denotes an interpolation operator.

We assume that the smoothed porosity $\mathcal{S}(\eta_h^n)$ is sufficiently regular such that there exists a constant dependent on $\mathcal{S}(\cdot)$, $C_{\mathcal{S}(\eta_h^n)}$ such that

$$\|\mathcal{S}(\eta_h^n) - I_h \mathcal{S}(\eta_h^n)\|_{L^\infty(\Omega)} = \|\mathcal{S}(\eta_h^n) - \eta_h^{n,s}\|_{L^\infty(\Omega)} \leq C_{\mathcal{S}(\eta_h^n)} h^{m+1}. \quad (4.15)$$

The precise dependence of $C_{\mathcal{S}(\eta_h^n)}$ on $\mathcal{S}(\cdot)$ will depend on the particular smoother used.

The computability of the approximation scheme (4.11)-(4.13) is established in the following lemma.

Lemma 4.1 *There exists a unique solution $(\mathbf{u}_h^n, p_h^n, \eta_h^n) \in (X_h, Q_h, R_h)$ satisfying (4.11)-(4.13).*

Proof: For $\{\phi_j\}_{j=1}^{N_R}$ a basis for R_h , and $\eta_h^n = \sum_{j=1}^{N_R} c_j \phi_j$, equation (4.13) is equivalent to $\mathbf{A}\mathbf{c} = \mathbf{d}$, where $\mathbf{c} = [c_1, c_2, \dots, c_{N_R}]^T$, and for $i, j = 1, 2, \dots, N_R$,

$$A_{ij} = \left(\left(\frac{1}{\Delta t} + \frac{1}{2} g(|\tilde{\mathbf{u}}_h^n + \mathbf{b}^{n-1/2}|) \right) \phi_j, \phi_i \right), \quad \text{and} \quad \mathbf{d}_i = \int_{\Omega} \left(\frac{1}{\Delta t} - \frac{1}{2} g(|\tilde{\mathbf{u}}_h^n + \mathbf{b}^{n-1/2}|) \right) \eta_h^{n-1} \phi_i d\Omega.$$

Note that as $\mathbf{A}\mathbf{c} = \mathbf{0} \Rightarrow \mathbf{c}^T \mathbf{A}\mathbf{c} = 0$

$$\begin{aligned} \Leftrightarrow \int_{\Omega} \left(\frac{1}{\Delta t} + \frac{1}{2} g(|\tilde{\mathbf{u}}_h^n + \mathbf{b}^{n-1/2}|) \right) \eta_h^n \eta_h^n d\Omega = 0 &\Rightarrow \eta_h^n = 0 \\ &\Rightarrow \mathbf{c} = \mathbf{0}, \end{aligned}$$

it follows that the (square) linear system (4.13) has a unique solution for η_h^n .

Given η_h^n and $\mathbf{A}\beta\mathbf{2}$, the existence and uniqueness of $(\mathbf{u}_h^n, p_h^n) \in X_h \times Q_h$ is well known from the approximation theory of Darcy fluid flow equations. ■

Theorem 4.1 *For (\mathbf{u}, p, η) satisfying (4.1)-(4.3) and (4.6)-(4.9), and $(\mathbf{u}_h^n, p_h^n, \eta_h^n)$ satisfying (4.11)-(4.13), and assuming that $C_{\mathcal{S}(\eta_h^n)}$ given in (4.15) is bounded by $C_{\mathcal{S}} \|\eta^n\|_{m+1}$, we have that for Δt sufficiently small there exists $C > 0$ independent of the h and Δt , such that for $n = 1, 2, \dots, N$,*

$$\|\mathbf{u}^n - \mathbf{u}_h^n\|_X + \|p^n - p_h^n\| + \|\eta^n - \eta_h^n\| \leq C \left((\Delta t)^2 + h^{k+1} + h^{m+1} \right). \quad (4.16)$$

Outline of the proof: The complete details of the proof are given in [8]. Here we briefly summarize the key steps in the proof.

Step 0. Notation.

For \mathcal{U}^n, τ^n in Z_h and R_h , respectively, let

$$\begin{aligned} \mathbf{\Lambda}^n &= \mathbf{u}^n - \mathcal{U}^n, & \mathbf{E}^n &= \mathcal{U}^n - \mathbf{u}_h^n \\ \psi^n &= \eta^n - \tau^n, & F^n &= \tau^n - \eta_h^n \\ \varepsilon_{\mathbf{u}} &= \mathbf{u}^n - \mathbf{u}_h^n, & \varepsilon_{\eta} &= \eta^n - \eta_h^n. \end{aligned} \quad (4.17)$$

Step 1. Derive and estimate for $\|\mathbf{E}^n\|$.

Beginning with (4.11) and (3.1) we obtain

$$\beta_{\min}\|\mathbf{E}^n\| \leq \beta_{\text{Lip}}\|\mathbf{u}^n + \mathbf{b}^n\|_{\infty}\|\eta_h^{n,s} - \eta^{n,s}\| + \beta_{\max}\|\mathbf{\Lambda}^n\|. \quad (4.18)$$

Step 2. Estimate for $\|\eta_h^{n,s} - \eta^{n,s}\|$.

With the triangle inequality,

$$\begin{aligned} \|\eta_h^{n,s} - \eta^{n,s}\| &\leq \|\eta_h^{n,s} - \mathcal{S}(\eta_h^n)\| + \|\mathcal{S}(\eta_h^n) - \eta^{n,s}\| \leq \|\eta_h^{n,s} - \mathcal{S}(\eta_h^n)\| + |\Omega|^{1/2}C_s\|\eta_h^n - \eta^n\| \\ &\leq \|\eta_h^{n,s} - \mathcal{S}(\eta_h^n)\| + |\Omega|^{1/2}C_s(\|\psi^n\| + \|F^n\|). \end{aligned} \quad (4.19)$$

Step 3. Derive an estimate for $\|F^n\|^2 - \|F^{n-1}\|^2$.

Beginning with (4.13) and (3.3) we obtain

$$\begin{aligned} \|F^n\|^2 - \|F^{n-1}\|^2 &\leq \Delta t\|d_t\psi^n\|^2 + 2\Delta t g_{\text{Lip}}^2\|\bar{\eta}^n\|_{\infty}^2(\|\tilde{\mathbf{E}}^n\|^2 + \|\tilde{\mathbf{\Lambda}}^n\|^2) + 2\Delta t g_{\text{max}}^2\|\bar{\psi}^n\|^2 \\ &\quad + \Delta t(6 + 2g_{\text{max}}^2)\|\bar{F}^n\|^2 + \Delta t R^n(\mathbf{u}, \eta), \end{aligned} \quad (4.20)$$

where

$$\begin{aligned} R^n(\mathbf{u}, \eta) &= \|d_t\eta^n - \frac{\partial\eta^{n-1/2}}{\partial t}\|^2 + g_{\text{Lip}}^2\|\bar{\eta}^n\|_{\infty}^2\|\tilde{\mathbf{u}}^n - \mathbf{u}^{n-1/2}\|^2 \\ &\quad + g_{\text{max}}^2\|\bar{\eta}^n - \eta^{n-1/2}\|^2. \end{aligned} \quad (4.21)$$

Step 4. Derive a bound for $\|F^\ell\|^2$.

Summing (4.20) from $n = 3$ to $n = l$, and using the discrete Gronwall's lemma [15, 16], we obtain, with constants $C, C_S, w_1, w_2, w_4, w_5$,

$$\begin{aligned} \|F^\ell\|^2 &\leq K\left(w_1Ch^{2k+2}\|\mathbf{u}\|_{k+1}^2 + (w_2C + w_4C_S^2)h^{2m+2}\|\eta\|_{m+1}^2\right. \\ &\quad + Ch^{2m+2}\int_{t_2}^{t_\ell}\|\eta_t\|_{m+1}^2 dt + (\Delta t)^4 w_5\int_0^{t_{\ell-2}}\|\mathbf{u}_{tt}\|^2 dt + \|F^2\|^2 \\ &\quad \left. + (\Delta t)^4\frac{g_{\text{max}}^2}{48}\int_{t_2}^{t_\ell}\|\eta_{tt}\|^2 dt + \frac{(\Delta t)^4}{1280}\int_{t_2}^{t_\ell}\|\eta_{ttt}\|^2 dt\right). \end{aligned} \quad (4.22)$$

Step 5. Derive a bound for $\|E^\ell\|^2$.

Combining (4.22) with (4.19) and (4.18) we obtain a bound for $\|E^\ell\|^2$.

Step 6. Error bounds for $\|\mathbf{u}^\ell - \mathbf{u}_h^\ell\|^2$ and $\|\eta^\ell - \eta_h^\ell\|^2$.

The error bounds for $\|\mathbf{u}^\ell - \mathbf{u}_h^\ell\|^2$ and $\|\eta^\ell - \eta_h^\ell\|^2$ then follow from the bounds for $\|E^\ell\|^2, \|F^\ell\|^2$, assumption (4.10), and using

$$\|\mathbf{u}^\ell - \mathbf{u}_h^\ell\|^2 \leq 2(\|\mathbf{E}^\ell\|^2 + \|\mathbf{\Lambda}^\ell\|^2), \quad \|\eta^\ell - \eta_h^\ell\|^2 \leq 2(\|F^\ell\|^2 + \|\psi^\ell\|^2).$$

Step 7. Error bound for $\|p^n - p_h^n\|$.

The error bound for $\|p^n - p_h^n\|$ is obtained by firstly using the discrete inf-sup condition

$$0 < c_0 \leq \inf_{q \in Q_h} \sup_{\mathbf{v} \in X_h} \frac{(q, \nabla \cdot \mathbf{v})}{\|q\| \|\mathbf{v}\|_X}$$

to show that for an arbitrary element $\mathcal{Q}^n \in Q_h$,

$$\begin{aligned} c_0 \|p_h^n - \mathcal{Q}^n\| &\leq \sup_{\mathbf{v} \in X_h} \frac{(p_h^n - \mathcal{Q}^n, \nabla \cdot \mathbf{v})}{\|\mathbf{v}\|_X} = \sup_{\mathbf{v} \in X_h} \frac{(p_h^n, \nabla \cdot \mathbf{v}) - (\mathcal{Q}^n, \nabla \cdot \mathbf{v})}{\|\mathbf{v}\|_X} \\ &\leq \beta_{\max} \|\mathbf{u}_h^n - \mathbf{u}^n\| + \beta_{\text{Lip}} \|\mathbf{u}^n + \mathbf{b}^n\|_{\infty} \|\eta_h^{n,s} - \eta^{n,s}\| + \|p^n - \mathcal{Q}^n\|. \end{aligned}$$

The estimate in (4.16) then follows from interpolation properties of Q_h and the triangle inequality,

$$\|p^n - p_h^n\| \leq \|p^n - \mathcal{Q}^n\| + \|p_h^n - \mathcal{Q}^n\|,$$

■

5 Numerical Computations

In this section we present four numerical examples to illustrate the numerical approximation scheme (4.11)-(4.13). Examples 1 and 2, for which we have an exact solution, are chosen to investigate the derived a priori error estimate for the approximation (4.16), and the dependence of the approximation on the smoother. Examples 3 and 4 use the numerical approximation scheme to investigate the performance of several filters.

Computations were performed using the `deal.II` software package [3]. For the 2-D computations (Examples 1 and 2) the domain was partitioned into quadrilaterals, and for Examples 3 and 4 the domain was partitioned into hexahedrons, $\Omega = \cup_{K \in \mathcal{T}_h} K$. We let $discP_k = \{f : f|_K \in \mathbb{P}_k^Q, \forall K \in \mathcal{T}_h\}$, and $contP_k = \{f \in C^0(\Omega) : f|_K \in \mathbb{P}_k^Q, \forall K \in \mathcal{T}_h\}$, see (4.5).

Example 1 and Example 2.

We consider $\Omega = (-1, 1) \times (0, 1)$ and approximate (3.1)-(3.3) for $t \in (0, 0.5]$. The true solution for the velocity and pressure is given by

$$\mathbf{u} = \begin{bmatrix} txy - t^2y^2 \\ tx + t^2x^2 - ty^2/2 \end{bmatrix}, \quad p(x, y) = 2t^2x - ty^2.$$

The function g that appears in the deposition function is set to $g(|\mathbf{u}|) = |\mathbf{u}|^2 + 1$. Assuming that the error in the numerical approximations is of order $\mathcal{O}(\Delta t^2 + h^{k+1})$ (see (4.16)), we chose $(\Delta t)^2 \propto h^{k+1}$.

For a function f and its approximations, $f_{h_1}^n, f_{h_2}^n$, computed on partitions on Ω with mesh parameters h_1 and h_2 , we defined the numerical convergence rate $r_{\|\cdot\|}$ as:

$$r_{\|\cdot\|} := \frac{\log(\|f(N\Delta t) - f_{h_1}^N\| / \|f(N\Delta t) - f_{h_2}^N\|)}{\log(h_1/h_2)}.$$

The quantity $r_{\|\cdot\|}$ is defined similarly.

Two different smoothers were investigated. For the first one, we computed the smoothed porosity η^s using a local averaging procedure. Specifically,

$$\eta^s(\mathbf{x}) = \frac{1}{|V(\mathbf{x})|} \int_{V(\mathbf{x})} \eta(\mathbf{x}) d\Omega,$$

where $|V(\mathbf{x})| = \delta$ denotes the area (volume) of the averaging domain $V(x)$.

The second smoother used was the differential smoother

$$\begin{aligned} -\delta\Delta\eta^s + \eta^s &= \eta \text{ in } \Omega \\ \eta^s &= \eta \text{ on } \partial\Omega. \end{aligned}$$

For both smoothers we used for the value of δ , $\delta = 0.05$.

Example 1.

For this example we take $\eta(x, y) = 0.8 - 0.5t^2xy$ and $\beta(\eta) = \eta^2 + 0.1$. Computations using the local averaging smoother, with $(\mathbf{u}_h, p_h, \eta_h, \eta_h^s) \in (RT_0, discP_0, discP_0, contP_1)$, and $(\mathbf{u}_h, p_h, \eta_h, \eta_h^s) \in (RT_1, discP_1, discP_1, contP_1)$, in the $\|\cdot\|$ norm are presented in Tables 5.1, and 5.2, respectively. Similar results were also obtained using the $\|\cdot\|$ norm, and when using the differential smoother.

The numerical convergence rates are consistent with those predicted by Theorem 4.1.

h	Δt	$\ \mathbf{u}(T) - \mathbf{u}_h(T)\ _X$	$r_{\ \cdot\ }$	$\ p(T) - p_h(T)\ $	$r_{\ \cdot\ }$	$\ \eta(T) - \eta_h(T)\ $	$r_{\ \cdot\ }$
1/2	2^{-3}	1.241E-01	1.22	1.176E-01	1.31	1.387E-03	0.86
1/4	$2^{-7/2}$	5.346E-02	0.78	4.759E-02	0.69	7.664E-04	0.49
1/8	2^{-4}	3.124E-02	1.05	2.946E-02	1.07	5.474E-04	1.08
1/16	$2^{-9/2}$	1.507E-02	0.95	1.403E-02	0.93	2.583E-04	0.81
1/32	2^{-5}	7.814E-03	1.05	7.366E-03	1.07	1.473E-04	1.19
1/64	$2^{-11/2}$	3.770E-03	-	3.507E-03	-	6.453E-05	-
Predicted convergence rate (see (4.16)): 1							

Table 5.1: Example 1: Convergence rates for $(\mathbf{u}_h, p_h, \eta_h, \eta_h^s) \in (RT_0, discP_0, discP_0, contP_1)$.

h	Δt	$\ \mathbf{u}(T) - \mathbf{u}_h(T)\ _X$	$r_{\ \cdot\ }$	$\ p(T) - p_h(T)\ $	$r_{\ \cdot\ }$	$\ \eta(T) - \eta_h(T)\ $	$r_{\ \cdot\ }$
1	2^{-3}	1.529E-02	1.55	9.882E-03	1.78	8.720E-04	0.99
1/2	2^{-4}	5.209E-03	1.80	2.882E-03	1.90	4.379E-04	1.78
1/4	2^{-5}	1.495E-03	1.91	7.721E-04	1.95	1.279E-04	1.91
1/8	2^{-6}	3.990E-04	1.95	1.995E-04	1.98	3.402E-05	1.96
1/16	2^{-7}	1.030E-04	-	5.067E-05	-	8.743E-06	-
Predicted convergence rate (see (4.16)): 2							

Table 5.2: Example 1: Convergence rates for $(\mathbf{u}_h, p_h, \eta_h, \eta_h^s) \in (RT_1, discP_1, discP_1, contP_1)$.

Example 2.

In this example we demonstrate the importance of smoothing the porosity input into the $\beta(\cdot)$ function. Using a perturbed porosity field $\eta = 0.8 - 0.5t^2xy + 0.03125 \sin(169x) \cos(169y)$ (see

Figure 5.1), and with $\beta(\cdot)$ given by (see Figure 5.2)

$$\beta(s) = \begin{cases} 9.1, & 0 \leq s < 0.1 \\ -8.5s + 9.95, & 0.1 \leq s < 0.3 \\ 7.4, & 0.3 \leq s < 0.4 \\ -8.5s + 10.8, & 0.4 \leq s < 0.6 \\ 5.7, & 0.6 \leq s < 0.7 \\ -18.5s + 18.65, & 0.7 \leq s < 0.9 \\ 2.0, & 0.9 \leq s \leq 1.0, \end{cases}$$

we study the convergence rates for two different cases. First, without smoothing the porosity input into the $\beta(\cdot)$ function (see Table 5.3), and then with a smoothed porosity input into $\beta(\cdot)$ (see Table 5.4).

For this example we used the differential smoother with $\delta = 0.05$.

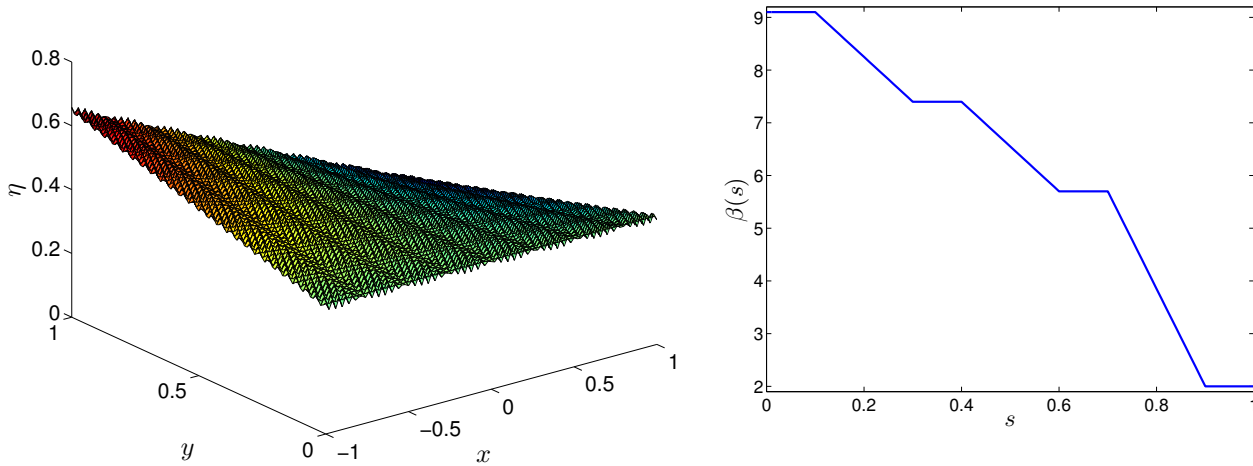


Figure 5.2: Plot of $\beta(s)$, Ex.2.

Figure 5.1: Porosity field for Ex. 2 at time $t = 0.5$.

$(\mathbf{u}_h, p_h, \eta_h) \in (RT_0, discP_0, discP_0)$							
h	Δt	$\ \mathbf{u}(T) - \mathbf{u}_h(T)\ _X$	$r_{\ \cdot\ }$	$\ p(T) - p_h(T)\ $	$r_{\ \cdot\ }$	$\ \eta(T) - \eta_h(T)\ $	$r_{\ \cdot\ }$
1/2	2^{-3}	1.674E-01	1.31	1.756E-01	1.43	1.976E-03	1.08
1/4	$2^{-7/2}$	6.742E-02	0.70	6.534E-02	0.84	9.324E-04	-0.79
1/8	2^{-4}	4.153E-02	1.06	3.640E-02	1.15	1.612E-03	0.66
1/16	$2^{-9/2}$	1.994E-02	0.31	1.636E-02	0.99	1.017E-03	-0.10
1/32	2^{-5}	1.611E-02	-	8.210E-03	-	1.091E-03	-
Convergence is not guaranteed by the theory.							

Table 5.3: Example 2: Convergence rates at $T = 0.5$, without smoothing the porosity.

The results in Table 5.3 indicate that without smoothing the convergence rate of the velocity drops drastically and the porosity does not converge. In contrast, using the smoothed porosity as input to $\beta(\cdot)$ the obtained approximations are convergent.

$(\mathbf{u}_h, p_h, \eta_h, \eta_h^s) \in (RT_0, discP_0, discP_0, contP_1)$							
h	Δt	$\ \mathbf{u}(T) - \mathbf{u}_h(T)\ _X$	$r_{\ \cdot\ }$	$\ p(T) - p_h(T)\ $	$r_{\ \cdot\ }$	$\ \eta(T) - \eta_h(T)\ $	$r_{\ \cdot\ }$
1/2	2^{-3}	1.671E-01	1.30	1.759E-01	1.42	2.202E-03	1.46
1/4	$2^{-7/2}$	6.786E-02	0.88	6.562E-02	0.85	8.013E-04	0.32
1/8	2^{-4}	3.691E-02	1.08	3.638E-02	1.15	6.410E-04	0.24
1/16	$2^{-9/2}$	1.746E-02	0.96	1.640E-02	0.99	5.432E-04	0.74
1/32	2^{-5}	8.980E-03	-	8.235E-03	-	3.259E-04	-
Predicted convergence rate: 1							

Table 5.4: Example 2: Convergence rates at $T = 0.5$, using a smoothed porosity.

Example 3 and Example 4.

We consider $\Omega = (-1, 1) \times (0, 1) \times (0, 1)$ and approximate (3.1)-(3.3) for $t \in (0, 1]$. No flux boundary conditions, $\mathbf{u} \cdot \mathbf{n} = 0$, were imposed on the walls $x = -1$, $x = 1$, $y = -1$, $y = 1$, and a zero pressure condition, $p = 0$, on the outflow boundary $z = -1$.

Four filters, labelled **I** - **IV**, with different initial porosity profiles were investigated, all having the same initial non void space, $\nu(0)$, where

$$\nu(t) = \int_{\Omega} (1 - \eta(\mathbf{x}, t)) d\Omega.$$

The computational parameters used were $\Delta t = 2^{-5}$ and $h = 0.1$.

The initial porosity profiles in Filters **A** - **H**, see Figures 5.3 - 5.6, were

I: The porosity uniform distributed throughout the domain Ω .

II: The porosity increases radially in a continuous fashion.

III: The porosity decreases radially in a continuous fashion.

IV: The porosity decreases continuously in the positive z direction.

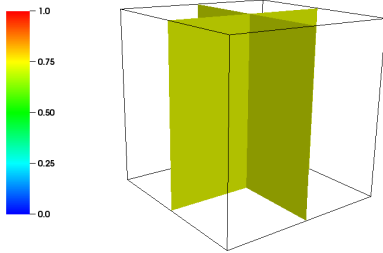


Figure 5.3: Filter I: Initial porosity field.

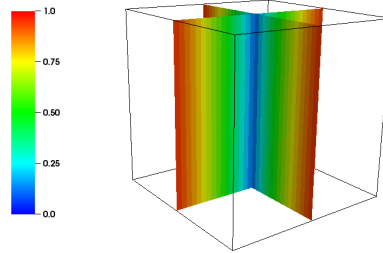


Figure 5.4: Filter II: Initial porosity field.

Example 3.

For Example 3 we consider the case of a specified inflow velocity for the fluid, namely $\mathbf{u} \cdot \mathbf{n} = -f$

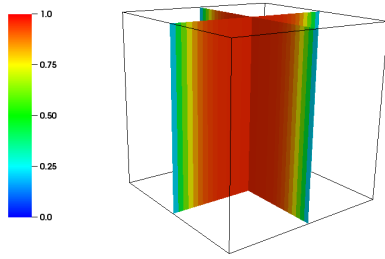


Figure 5.5: Filter III: Initial porosity field.

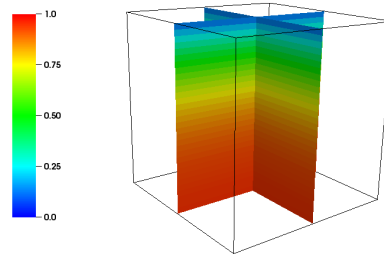


Figure 5.6: Filter IV: Initial porosity field.

on $z = 1$, where

$$f(\mathbf{x}, t) = (1 - x^2)(1 - y^2) \min \{1, 4t\} ,$$

and compare the non void space within each filter at time $T = 1$. Also measure is the maximum pressure within each filter at $T = 1$. The results are presented in Table 5.5. Plots of the final porosity fields for the filters are presented in Figures 5.7 - 5.10.

Filter	Nonvoid space $\nu(1)$	Max. pressure
I	5.34	7.40
II	5.41	11.00
III	5.50	7.03
IV	5.33	14.07

Table 5.5: Example 3: Non void space $\nu(t)$, and maximum pressure within each filter at $T = 1$.

In terms of the particulate deposited, all the filters' performances were very similar with a difference between filters of less than 2.5%. However there was a significant difference in term of the maximum pressure within each filter at $T = 1$, with a maximum value of 14.07 (Filter IV) and a minimum value of 7.03 (Filter III).

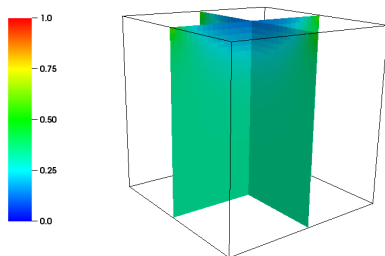


Figure 5.7: Filter I: Porosity field at $T = 1$.

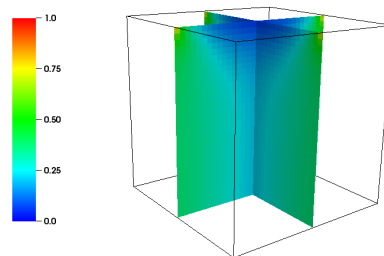


Figure 5.8: Filter II: Porosity field at $T = 1$.

Example 4.

In this example a inflow pressure, p_{in} , was specified and then the non void space within each filter at $T = 1$ was calculated, together with the total fluid flow through the filter. The inflow pressure

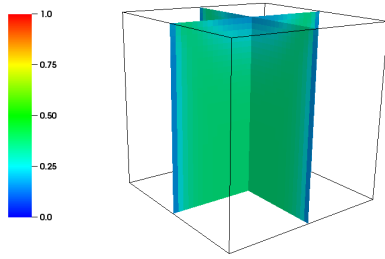


Figure 5.9: Filter III: Porosity field at $T = 1$.

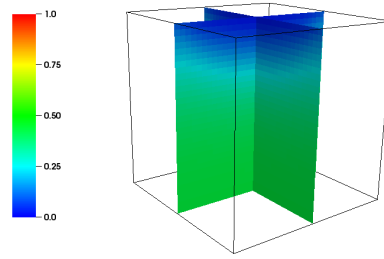


Figure 5.10: Filter IV: Porosity field at $T = 1$.

used was

$$p(\mathbf{x}, t) = 10 \min \{1, 4t\}.$$

The results are given in Table 5.6.

Filter	Non void space $\nu(1)$	Total flow
I	6.61	5.74
II	6.64	5.65
III	6.66	5.56
IV	6.34	5.02

Table 5.6: Example 4: Non void space at $T = 1$, and total flow from $t = 0$ to $t = 1$.

Similar to Example 3, the deposition within the filters was comparable, differing by less than 6%. The total flow however differed by more than 10% with the highest total flow of 5.74 occurring for filter I and the lowest total flow of 5.02 occurring for filter IV.

References

- [1] G. Allaire. Homogenization of the Navier-Stokes equations with a slip boundary condition. *Comm. Pure Appl. Math.*, 44(6):605–641, 1991.
- [2] M. Azaïez, F. Ben Belgacem, C. Bernardi, and N. Chorfi. Spectral discretization of Darcy’s equations with pressure dependent porosity. *Appl. Math. Comput.*, 217(5):1838–1856, 2010.
- [3] W. Bangerth, T. Heister, L. Heltai, G. Kanschat, M. Kronbichler, M. Maier, B. Turcksin, and T. Young. The dealii library, version 8.2. *Archive of Numerical Software*, 3(1), 2015.
- [4] S. Bartels, M. Jensen, and R. Müller. Discontinuous Galerkin finite element convergence for incompressible miscible displacement problems of low regularity. *SIAM J. Numer. Anal.*, 47(5):3720–3743, 2009.
- [5] J. Bear. *Dynamics of fluids in porous media*. Environmental Science series (New York). American Elsevier, 1972.

- [6] F. Brezzi and M. Fortin. *Mixed and hybrid finite element methods*. Springer-Verlag, New York, 1991.
- [7] Z. Chen and R. Ewing. Mathematical analysis for reservoir models. *SIAM J. Math. Anal.*, 30(2):431–453, 1999.
- [8] V.J. Ervin, H. Lee, and J. Ruiz-Ramirez. Nonlinear Darcy fluid flow with deposition. Technical Report, Clemson University No. TR2015_7_ve.hl.jr. (Available at http://www.clemson.edu/ces/math/dept_publications.html), 2015.
- [9] V.J. Ervin, H. Lee, and A.J. Salgado. Generalized Newtonian fluid flow through a porous medium. *J. Math. Anal. Appl.*, 433(1):603–621, 2016.
- [10] X. Feng. On existence and uniqueness results for a coupled system modeling miscible displacement in porous media. *J. Math. Anal. Appl.*, 194(3):883–910, 1995.
- [11] G.P. Galdi. *An Introduction to the Mathematical Theory of the Navier-Stokes Equations, Vol. 1*. Springer-Verlag, New York, 1994.
- [12] J. Galvis and M. Sarkis. Non-matching mortar discretization analysis for the coupling Stokes–Darcy equations. *Electron. Trans. Numer. Anal.*, 26:350–384, 2007.
- [13] V. Girault, F. Murat, and A. Salgado. Finite element discretization of Darcy’s equations with pressure dependent porosity. *M2AN Math. Model. Numer. Anal.*, 44(6):1155–1191, 2010.
- [14] J.K. Hale. *Ordinary differential equations*. Wiley-Interscience [John Wiley & Sons], New York-London-Sydney, 1969. Pure and Applied Mathematics, Vol. XXI.
- [15] J.G. Heywood and R. Rannacher. Finite-element approximation of the nonstationary Navier-Stokes problem. IV. Error analysis for second-order time discretization. *SIAM J. Numer. Anal.*, 27(2):353–384, 1990.
- [16] W. Layton. *Introduction to the numerical analysis of incompressible viscous flows*, volume 6 of *Computational Science & Engineering*. Society for Industrial and Applied Mathematics (SIAM), Philadelphia, PA, 2008.
- [17] K.R. Rajagopal. On a hierarchy of approximate models for flows of incompressible fluids through porous solids. *Math. Models Methods Appl. Sci.*, 17(2):215–252, 2007.
- [18] B.M. Rivière and N.J. Walkington. Convergence of a discontinuous Galerkin method for the miscible displacement equation under low regularity. *SIAM J. Numer. Anal.*, 49(3):1085–1110, 2011.
- [19] L. Traverso, T.N. Phillips, and Y. Yang. Mixed finite element methods for groundwater flow in heterogeneous aquifers. *Computers & Fluids*, 88:60–80, 2013.
- [20] S. Whitaker. Flow in porous media I. A theoretical derivation of Darcy’s law. *Transp. Porous Media*, 1:3–25, 1986.